LAWRENCE
LIVERMORE
NATIONAL
LABORATORY

UCRL-JRNL-228395

Dynamic Diamond Anvil Cell (dDAC): A novel device for studying the dynamic-pressure properties of materials

W. J. Evans, C-S. Yoo, G. W. Lee, H. Cynn, M. J. Lipp, K. Visbeck

February 27, 2007

Review of Scientific Instruments

Dynamic Diamond Anvil Cell (dDAC): A novel device for studying the dynamic-pressure properties of materials

William J. Evans, Choong-Shik Yoo, Geun Woo Lee, Hyunchae Cynn, Magnus J. Lipp, Ken Visbeck

Abstract

We have developed a unique device, a dynamic diamond anvil cell (dDAC), which repetitively applies a time-dependent load/pressure profile to a sample. This capability allows studies of the kinetics of phase transitions and metastable phases at compression (strain) rates of up to 500 GPa/sec (~0.16 s^{-1} for a metal). Our approach adapts electro-mechanical piezoelectric actuators to a conventional diamond anvil cell design, which enables precise specification and control of a time-dependent applied load/pressure. Existing DAC instrumentation and experimental techniques are easily adapted to the dDAC to measure the properties of a sample under the varying load/pressure conditions. This capability addresses the sparsely studied regime of dynamic phenomena between static research (diamond anvil cells and large volume presses) and dynamic shock-driven experiments (gas guns, explosive and laser shock). We present an overview of a variety of experimental measurements that can be made with this device.

I. Introduction

We describe a novel device, the dynamic diamond anvil cell (dDAC), which uses electro-mechanical actuators to apply a load, producing a tailored time-dependent pressure profile on a sample. The applied load is driven by a function generator and can be set to virtually any waveform, including step functions, ramps and smoothly varying sinusoids. The repetitive nature of the applied load permits synchronization with a time-resolved probe allowing signal averaging and enhancement of the quality of the measurement (signal to noise). At moderate compression rates, time-resolved measurements can be made using a chopper to shutter conventional diamond anvil cell optical and x-ray diagnostics. The dDAC is a unique capability permitting time-dependent observations and detailed studies of pressure-induced phase transitions, such as melting and crystallization. Time-resolved approaches present the possibility of studying the kinetics of transitions. We describe the dDAC device, materials considerations, operational limitations, experimental configurations and early experimental results.

Dynamic phenomena of non-metals at finite compression rates (<10^5 s^{-1}) slower than that of high-speed impact processes (shocks - gas gun, laser, magnetic) are a largely unexplored regime. Modest strain rates can drive systems out of chemical equilibrium and induce transformations to metastable local minimum energy configurations. Processes in this regime include molecular phase transformations, such as the kinetics of crystallization and growth in liquid-solid transitions. The physics of these processes is relevant to a broad range of technological and geophysical processes.[1-5] A detailed understanding of pressure-induced crystal growth rates and morphologies would be extremely valuable to optimizing growth of superhard-materials such as cubic-BN and

diamond. Further, such information would also yield insights into mineral growth processes and dynamics within the Earth. Indeed the influence of variable compression rates is unknown for most phase transformations. Compression rates can lead to kinetically impeded transformations and even the formation of metastable phases.[6, 7] To study the influence of compressions rates on the physical properties of materials, we have developed a novel device, called the dynamic Diamond Anvil Cell (dDAC).

High-pressure experimental science has traditionally been split between two very different approaches, static and dynamic. Dynamic or shock experiments probe the properties of materials at high pressures by accelerating the material through a drive or impact it with a projectile.[8] Measurements of the resultant shock wave and particle velocity, followed by analysis using the Rankine-Hugoniot equations, permit the determination of a variety of properties including density, pressure and enthalpy. These are very rapid experiments, lasting no more than a few microseconds, and are capable of achieving very high pressures (several 100 GPa) and very high temperatures (several 1000 Kelvins). Shock experiments face several challenges imposed by the limited diagnostics suitable for the short time interval of the event, its single-shot nature, and the adiabatic condition that leads to relatively high temperatures. In contrast, static experiments use opposed anvils to exert a fixed pressure on the sample under study. At pressure, the materials can be studied using a variety of non-invasive techniques including optical spectroscopy and x-ray scattering.[9, 10] In stark contrast to dynamic experiments, static experiments typically last for several days, with effectively unlimited time for data collection. The maximum pressures achievable are approximately 350 GPa, and the temperature can range from less than 1 Kelvin to a few thousand Kelvin. Static and dynamic experiments are powerful complimentary approaches that have progressed in parallel to advance a comprehensive scientific understanding of materials properties at high pressures. However, the difference in time scales and temperatures has hindered direct comparisons of experimental results. In this manuscript we describe the dDAC that we have developed, which aims to bridge the gap between static and dynamic experiments and address issues regarding the kinetics of transformations at high pressures. The kinetics of pressure-induced transitions at low-to-moderate compression rates have been largely unexplored because no experimental approaches existed to probe these phenomena. The dDAC is an important advance for studying this important and rich area of materials physics.

II. Experimental Development

A. Instrument design

The dDAC is an enhancement on the design of conventional diamond anvil cells (DAC). This approach allows us to use existing DAC ancillary instrumentation for loading samples and experimental studies. A simplified description of our dDAC design is a conventional DAC coupled to piezo-electric actuators that drive a load supplementing the main load provided by the conventional load screws. We further elaborate on the details of our design below.

Since the dDAC is derived from a conventional DAC design, a basic description of a DAC is a useful starting point for the description. Conventional DACs have been thoroughly reviewed in several manuscripts,[11-13] so our description here is brief. A DAC is a precision device for compressing a sample between two diamond anvils. The diamond anvils are typically brilliant cut diamonds with the tips truncated to a flat surface. The two diamonds are mounted in a piston-cylinder assembly that maintains sub-micron alignment of the anvils tips as the diamonds are driven together. Screws bridging the cylinder and piston components are tightened to drive the diamonds together and apply a load. The sample under study is captured between the diamonds and confined laterally by a metal gasket.

The dDAC enhances the basic DAC design by incorporating piezo-electric actuators that deviate the static load imposed by the screws. Cross-sectional and end-on views of the dDAC are shown in figure 1. Instead of a piston-cylinder we use a plate and a cylindrical block that maintain their alignment using guide-pins, a design similar to that of Merrill-Basset cells. As can be seen in the figure, there is a static load screw as used in conventional DACs and mounted parallel but on the opposite side of the DAC from the screw, is an electro-mechanical peizo-electric actuator. The screws apply a compressive load to the sample pressurizing the sample. The static load crews are mounted with Belleville spring washers. The piezo-electric actuators apply an expansive load, counteracting the screw load and reducing the load/pressure on the sample. The spring washers permit a few microns of travel between the two DAC body components. Thus, the change in load is accompanied by a small change in the diamond position and the associated gasket thickness. In our design we utilize three piezo-electric (pe) actuators (Piezo Jenna, Model PAHL 18/20) that are symmetrically distributed (120°) around the load axis of the dDAC. The dDAC body components (plate & cylindrical block) are machined from T304 stainless steel, and the anvil seats are either stainless steel or tungsten carbide. In order to be assured that the actuators apply their loads uniformly, brass keeper plugs are screwed in behind the actuators and tensioned equally. The pe actuators are driven using a waveform generator (Agilent, Model 33120A, 15 MHz Function/Arbitrary Waveform Generator) and a power supply/amplifier (Piezo Jenna, Model ENT400/ENV400) as shown in figure 2.

B. Operation Details

The operation of the dDAC is simple, though there are important subtleties of the operation. A detailed understanding of the performance strengths and limitations is crucial to effectively planning experiments and utilizing this instrument. We are beginning to understand these issues and discuss them below. A sample is loaded in a fashion entirely similar to procedures used for conventional DACs. A metal gasket is preindented to a thickness of 20-40 microns, depending on the targeted pressure range for experimentation. A sample is loaded into the gasket hole along with several ruby chips (for pressure calibration) and a suitable hydrostatic medium. The static load screws, analogous to the screws in a conventional DAC, are uniformly tightened and torqued until the maximum pressure to be accessed in the experiment is achieved. The three piezo-electric actuators are then inserted into holes in the cylindrical metal body of the dDAC and the keeper plugs are lightly tightened behind them to insure that there are no

gaps between the pe actuators and the dDAC. The function generator and amplifier are coupled in series to the pe actuators and the dDAC is ready for operation. An applied voltage causes the actuators to apply an expansive load on the dDAC. This load counteracts the compressive load from the load screws and decreases the effective load on the gasket/sample. This decrease in load reduces the pressure on the sample.

An important consideration is the selection of gasket material and gasket thickness. The pressure variation is achieved through the change in sample volume as the pe actuators alter the load on the sample; the change in volume causes a change in pressure, which can be measured using ruby fluorescence, for example. In order for the dDAC to reproducibly cycle the load/pressure, as required for signal averaging, the load variation must be confined to the gasket's elastic limit. If the load exceeds the elastic limit of the gasket, the gasket will be plastically deformed and the sample volume/pressure will not recover it initial volume. Further, the maximum elastic deformation of the gasket determines the maximum volume variation that can be achieved. The associated pressure change is determined by the change in volume and equation-of-state of the material contained in the dDAC. At a given pressure the maximum pressure change will be smaller for more compressible materials. In figure 3 we show the pressure change, Δp, that can be achieved for a given initial pressure, p, in the case of a water sample. The maximum pressure ramping rate we have observed is 500 GPa/sec, which is determined by the response time of our pe actuators, the equation-of-state of the sample and the mechanical response of the dDAC.

The mechanical response of the gasket material and the equation-of-state of the materials being studied determine the intrinsic maximum pressure range of the dDAC. Modeling the sample chamber as a cylinder and neglecting changes in the cross-sectional area of the sample we find,

$$\frac{\Delta V}{V} \approx \frac{A\Delta d}{Ad} = \frac{\Delta d}{d}$$

where, V is the volume of the sample chamber, A is the cross-sectional area of sample chamber, d is the sample thickness, and Δx is the maximum change in the parameter x (x=A or d) produced by the dDAC. The maximum value for $\Delta d/d$ is determined by the elastic response limit of the gasket. The maximum elastic response is an intrinsic feature of the gasket material. Maintaining the constant cross-sectional area assumption, the maximum percentage volume change of a sample is independent of the gasket thickness and is equal to the maximum elastic response of the gasket thickness. Assuming the elastic constants determined in tension are a reasonable approximation for purposes of this discussion, we find that for Rhenium (Young's Modulus 430 GPa, and Yield Stress 1800 MPa) the maximum strain is .004. Thus the maximum change in sample volume is 0.4%. Applying this increment to solid argon, for example, a 0.4% change in volume corresponds to a change in pressure of 0.05 GPa at 2.0 GPa, and 0.75 GPa at 50 GPa. For a stiffer material this pressure change will be larger. All materials stiffen at higher pressures, so the available pressure variation range will grow as the static pressure increases. If this limit is exceeded, the gasket will plastically deform and the pressure

profile will not be repeated. This is unacceptable for the experiments described here, since we signal average over several cycles and require the pressure profile of the dDAC to be reproducible. It should be noted that this discussion relies on several assumptions in regard to material properties and sample behavior. A more sophisticated analysis would yield better predictions, but we do not expect them to be significantly different.

The intrinsic performance characteristics of the pe actuators determine the limits of our dDAC studies. The maximum frequency response time of the pe actuautors we are using is ~1 μm/μsec. This determines the upper-bound of the strain rate we can impose on a sample. The actual maximum strain rate is even lower because of the mechanical response limitations (friction) of the dDAC. The maximum pressure ramping we have measured is 500 GPa/sec. We feel this can be significantly improved by using a high power amplifier power supply and enhanced pe actuators.

C. Time-resolved Diagnostics

Using time-resolved probes with the dDAC, we can measure dynamic changes in material properties during the compression and decompression. We have used a high-speed video camera (Photron APX-RS, 1024x1024 resolution, 2000 frames/sec) to image pressure-induced melting or freezing of the sample. Many conventional diagnostic techniques used in diamond anvil cell research (optical spectroscopy (Fluorescence, Raman, Broadband Visible) and x-ray scattering) are not suited to short exposure times. We address this by repetitively cycling the dDAC and signal averaging over the time interval in the pressure cycle of interest. Synchronizing a shuttered detector with the dDAC function generator drive permits a particular interval of interest in the dDAC loading/pressure cycle to be selectively interrogated, as shown schematically in figure 4. The function generator/shutter delay can be systematically increased to produce a series of snapshots of the entire pressure cycle. The fundamental limits of a mechanical shutter can be exceeded and extremely short interval measurements may be achieved by synchronizing the dDAC to pulsed high-power laser or x-ray sources.

The mechanical response of the chopper/shutter (Uniblitz LS6 and New Focus Model 3501) limits the current work to relatively slow duty cycles (40 Hz) and modest exposure times (>1 ms). The maximum duty cycle of the particular pe actuators used in our studies is 500 Hz, and the maximum response time is ~1 μm/μsec. However, the duty cycle is relatively inconsequential and only limits the pressure-cycle period.

Using this shutter-based approach we have measured the time/pressure-dependence of the pressure (ruby fluorescence), Raman shift and x-ray diffraction signal during cycling of the dDAC. Figure 5a shows time-resolved ruby fluorescence spectra of a water sample during pressure cycling in the dDAC. The data is shown as the pressure versus time (or pe actuator voltage) profile of figure 5b. Similarly, figure 6 shown Raman spectra of a nitrogen sample during pressure cycling in the dDAC. The Raman spectra show features of the pressure-induced δ–ε transition at room temperature in nitrogen. Coordinating the Raman and pressure measurements we are able to study the pressure bounds of the transformation. Tailored function generator drive functions for the pe actuators are crucial in distinguishing metastability from transformation kinetics. A function generator

drive waveform that ramps across the expected phase transformation pressure and then holds the pressure, allows us to determine whether the sample eventually converts (kinetically hindered) or remains in the phase indefinitely (metastable).

III. Applications

A. Metastable Phases

The unique controlled pressurization/loading capabilities of the dDAC enable pressure-temperature phase space excursions that can produce metastable phases. It is well known that subjecting materials to rapid pressurization and cooling rates can result in unique crystal structures.[14] Simplest to envision is the formation of amorphous phase from the rapidly cooled/solidified melts. Similarly, with sufficiently rapid cooling rates crystal structures can be captured and stabilized in known or novel structures well outside of their thermodynamic phase stability regions.

We have used the dDAC to study phase transformations and metastable phases of water.[15] At room temperature and thermodynamic equilibrium, water solidifies at 0.9 GPa into the ice-VI structure (tetragonal) and transforms to ice-VII (cubic) at 2.2 GPa. Using the dDAC to apply sufficiently rapid compression rates (>0.08 GPa/sec), we are able to supercompress water, maintaining it in the liquid phase up to ~1.8 GPa, well beyond the known thermodynamic liquid-solid phase line at 0.9 GPa and within the ice-VI thermodynamic stability field. Even more surprising, we find that the supercompressed water crystallizes into the ice-VII structure from the supercompressed liquid while still in the thermodynamic stability field of ice-VI. The Raman spectrum of the metastable ice-VII in the thermodynamic stability field of ice-VI is shown in figure 7. We have used this result to determine interfacial free energies of ice phases, and develop insights regarding the local structure of liquid water. This finding suggests that compression rates may lead to the formation of other metastable ice phases and our understanding of phase transformation lines and stability of molecular fluids and solids in general warrants further investigation.

B. Crystal Growth

Crystal growth is an area where the dDAC has a novel and important impact. Studies of macroscopic crystal growth parameters (e.g., crystal size and growth rate as a function of cooling/compressing rate and temperature/pressure) can be used to infer microscopic mechanisms of atomic or molecular mobility. Using the dDAC pressure-induced growth of crystals can be directly observed and the influence of the compression rate on the morphology and growth mechanisms can be studied. Traditionally crystal growth has been studied from the thermal perspective by varying the temperature or cooling rate. The dDAC permits an analogous approach using pressure. In contrast to thermal solidification, where rates are limited by thermal conductivity (0.58W/mK for water at STP), pressure-induced solidification can occur at rates several orders of magnitude faster, where the speed of sound (1500 m/s for water at STP) dictates the pressurization rate. In addition, there is no significant convective flow, and a homogeneous change in the chemical environment can be achieved by pressurization.

We have studied the crystallization of water using the dDAC and find a variety of different crystallization processes depending on the compression rate.[16] Our work complements previous shock investigations,[17-19] probing a lower strain rate regime than these previous studies. Although different, we find similarly rich phenomena. We have imaged the growth using high-speed videography and identified dramatic changes in the growth morphology and rate depending on the compression-rate. At low strain rates ($<0.89\ s^{-1}$, derived from the motion of the pe acutuator), we observed the growth of a well-formed faceted crystal shown in figure 8a. However, at higher compression rates, we observe dendritic crystal growth and surface instabilities that lead to extremely rapid growth rates. Figure 8b shows an image of a dendritic ice-VI crystal produced by driving the dDAC at a strain rate of $136\ s^{-1}$. We speculate that the very rich behavior of water and ice-VI will also be manifested in other molecular systems and mixtures. The growth of calthrate-ices in deep ocean waters containing NaCl and CO_2 may show similar behavior.

III. Discussion

Our development and use of the dDAC have demonstrated several new capabilities and suggest a wide range of possible studies encompassing phase transformation kinetics and strain rate dependent phenomena. Making simple modifications to conventional DAC designs, we incorporated pe modulators, which allow us to electronically control a time-dependent load on the sample. We have demonstrated the dDAC's capability of repetitively applying a prescribed loading profile to a sample and used time-resolved diagnostics to capture the progression of the sample's behavior. These capabilities have been applied to the study of water and nitrogen to examine phase transformation dynamics, growth of metastable phases and crystal growth rates and morphologies. These achievements mark an important advance in the ability to bridge the gap between conventional static-pressure diamond anvil cell experiments and dynamic shock-physics studies.

Our initial time-resolved studies have achieved new and important scientific results, yet further advances are possible through the use of more advanced instrumentation; heating/cooling elements, *in-situ* temperature sensors, and short pulse lasers and x-ray sources. The experiments described here have been conducted at room temperature. Incorporating heating and cooling elements will allow the very same types of studies to be conducted over a range of conditions and the temperature-dependence of transition kinetics and metastable phases can be investigated.

Such advances would be useful in investigating pressure-induced material processes. Pressure is known to be a powerful tool for altering interatomic and molecular potentials. The fine pressure control of the dDAC can provide a valuable capability for studies of protein denaturing and amorphization processes. Further, dynamic tuning of the pressure conditions for crystal growth can lead to controlled synthesis of nanoparticles.[20] Precise *in-situ* temperature sensors would be used to measure thermal changes associated with pressure-induced phase transitions, which are often accompanied by a latent heat. Finally advancing passed our use of a mechanical shutter (>1 ms exposure time) can lead to detection windows that are orders of magnitude shorter. Ultrafast time windows can be

achieved with femtosecond lasers (for Raman spectroscopy) or the 100 ps x-ray pulses of a third generation synchrotron source (for x-ray diffraction). We have conducted basic time-resolved x-ray diffraction experiments on iron operating the dDAC at the Argonne National Laboratory Advanced Photon Source and have demonstrated this capability. Further optimization is underway to utilize the single bunch synchrotron x-ray pulses. These very short pulses offer the opportunity of time-resolving the structural dynamics of pressure-induced melting and freezing transitions. The electronic drive of the dDAC is easily synchronized to these short-pulse sources offering novel insights into dynamic processes in nature.

IV. Summary and Conclusion

The dDAC is a new and important tool for studying dynamic phenomena, such as the kinetics of crystallization and the importance of compression rates on the stability and metastability of high-pressure phases. This simple device is suitable for use with many of the conventional DAC diagnostics and is easily adapted to time-resolved probes. Further use and development of this device will provide novel insights regarding dynamic phenomena and strain-rate dependencies. Our preliminary work demonstrates significant progress bridging the gap between conventional static and dynamic high-pressure science experiments.

Acknowledgements

This work was performed under the auspices of the U.S. DOE by the Univ. of California, Lawrence Livermore National Laboratory under contract No. W-7405-Eng-48. Portions of this work were performed at HPCAT (Sector 16), Advanced Photon Source (APS), Argonne National Laboratory. Use of the HPCAT facility was supported by DOE-BES, DOE-NNSA (CDAC), NSF, DOD –TACOM, and the W.M. Keck Foundation. Use of the APS was supported by DOE-BES, under Contract No. W-31-109-ENG-38. We gratefully acknowledge the assistance from Dr. H.-P. Liermann, Dr. W. Yang and Eric Rod at beamline 16BM-B.

[1] I. Martinez and P. Agrinier, Comptes Rendus De L Academie Des Sciences Serie Ii Fascicule A-Sciences De La Terre Et Des Planetes **327**, 75 (1998).

[2] P. F. McMillan, Nature **391**, 539 (1998).

[3] P. Peyre and R. Fabbro, Optical And Quantum Electronics **27**, 1213 (1995).

[4] P. F. McMillan, Nature Materials **4**, 715 (2005).

[5] S. Nemat-Nasser and J. Y. Choi, Acta Materialia **53**, 449 (2005).

[6] P. F. McMillan, Chemical Society Reviews **35**, 855 (2006).

[7] P. F. McMillan, High Pressure Research **23**, 7 (2003).

[8] G. E. Duvall and R. A. Graham, Reviews of Modern Physics **49**, 523 (1977).

[9] R. J. Hemley and H. K. Mao, Mineralogical Magazine **66**, 791 (2002).

[10] A. Jayaraman, Reviews of Modern Physics **55**, 65 (1983).

[11] D. M. Adams and A. G. Christy, High Temperatures-High Pressures **24**, 1 (1992).

[12] A. Jayaraman, Scientific American **250**, 54 (1984).

[13] A. Jayaraman, Review of Scientific Instruments **57**, 1013 (1986).

[14] U. Schubert and N. Husing, *Synthesis of Inorganic Materials* (Wiley-VCH, Weinheim, 2005).
[15] G. W. Lee, W. J. Evans, and C. S. Yoo, Physical Review B **74** (2006).
[16] G. W. Lee, W. J. Evans, and C.-S. Yoo, Proceedings of the National Academy of Science **2007**, accepted for publication (2007).
[17] D. H. Dolan, J. N. Johnson, and Y. M. Gupta, Journal Of Chemical Physics **123** (2005).
[18] D. H. Dolan and Y. M. Gupta, Journal Of Chemical Physics **121**, 9050 (2004).
[19] D. H. Dolan and Y. M. Gupta, Chemical Physics Letters **374**, 608 (2003).
[20] J. Liu, H. He, X. Jin, Z. Hao, and Z. Hu, Materials Research Bulletin **36**, 2357 (2001).

Figure Captions

Figure 1. dDAC design schematics showing body and piezo-electric (pe) actuators. a) Cross-sectional view showing cylindrical body above the plate with locations of pe actuators, static load screws anvils. b) End-on view showing positioning of pe actuators, static load screws and guide pins.

Figure 2. Schematic of dDAC operation showing instrumentation and connections including a shutter for time-resolved experiments.

Figure 3. Plot showing the dDAC pressure variation range at a given nominal pressure. The data are shown for a water sample (~100 μm diameter, 300 μm diamond flats). The slope of this curve will increase for stiffer (less compressible) materials.

Figure 4. Time-resolved synchronization scheme for selectively probing the loading/unloading cycle of a sample in the dDAC. The time delay, Δt, is selected by the digital delay/pulse generator and set to probe the desired range in the cycle. The drive waveform can be set as desired (ramp, step function, pulse) provided it is within the performance range of the pe actuators. A sinusoidal drive is shown.

Figure 5. Time-resolved ruby fluorescence spectra of a sample in the dDAC. The sample (water, stainless steel gasket, ~5 μm thick) is being driven by a sinusoidal waveform with a period of 20 seconds (0.05 Hz).
a) The raw ruby spectra (exposure time 100 msec). The gray background strip emphasizes the movement of the ruby R1 fluorescence line.
b) The pressure as a function of time. Square symbols are the pressure determined from the ruby specta. Lines between the squares are a guide to the eye, emphasizing the abrupt jump at 18 and 36 sec, and the dashed line is the voltage applied to the pe. The pressure shows a smooth variation between 0.15 and 1.4 GPa, expect for the kink in the rising edge, representative of the liquid-solid phase transition. Plateaus at 5 and 25 sec are representative of melting.

Figure 6. Time-resolved Raman spectra of a nitrogen sample in the dDAC showing the transition from the β-phase to the δ-phase. The pressure and elapsed time are written above the corresponding spectrum. The initial 4.2 GPa spectrum shows the pure β-phase Raman signal, β/δ coexistence at 4.9 GPa and pure δ-phase at 5.5 GPa. Spectra were collected using a trapezoidal drive waveform and a compression rate of 150 GPa/sec. The measurement exposure window was 1 ms and the signal averaged for 20 minute.

Figure 7. Raman spectra of water supercompressed at a rate of 0.16 GPa/s in the dDAC. Metastable ice-VII at 1.7 GPa was formed from supercompressed water. Both the supercompressed water and the resultant ice-VII are within the thermodynamic stability field of ice-VI.

Figure 8. Video images in transmission of ice-VI crystals grown in the dDAC. Diameter of sample hole is ~150 μm. a) A faceted well-formed ice VI crystal produced at strain rate of 0.89 s^{-1}. b) a dendritic crystal formed at a strain rate of 136 s^{-1}.

.

Figure 1

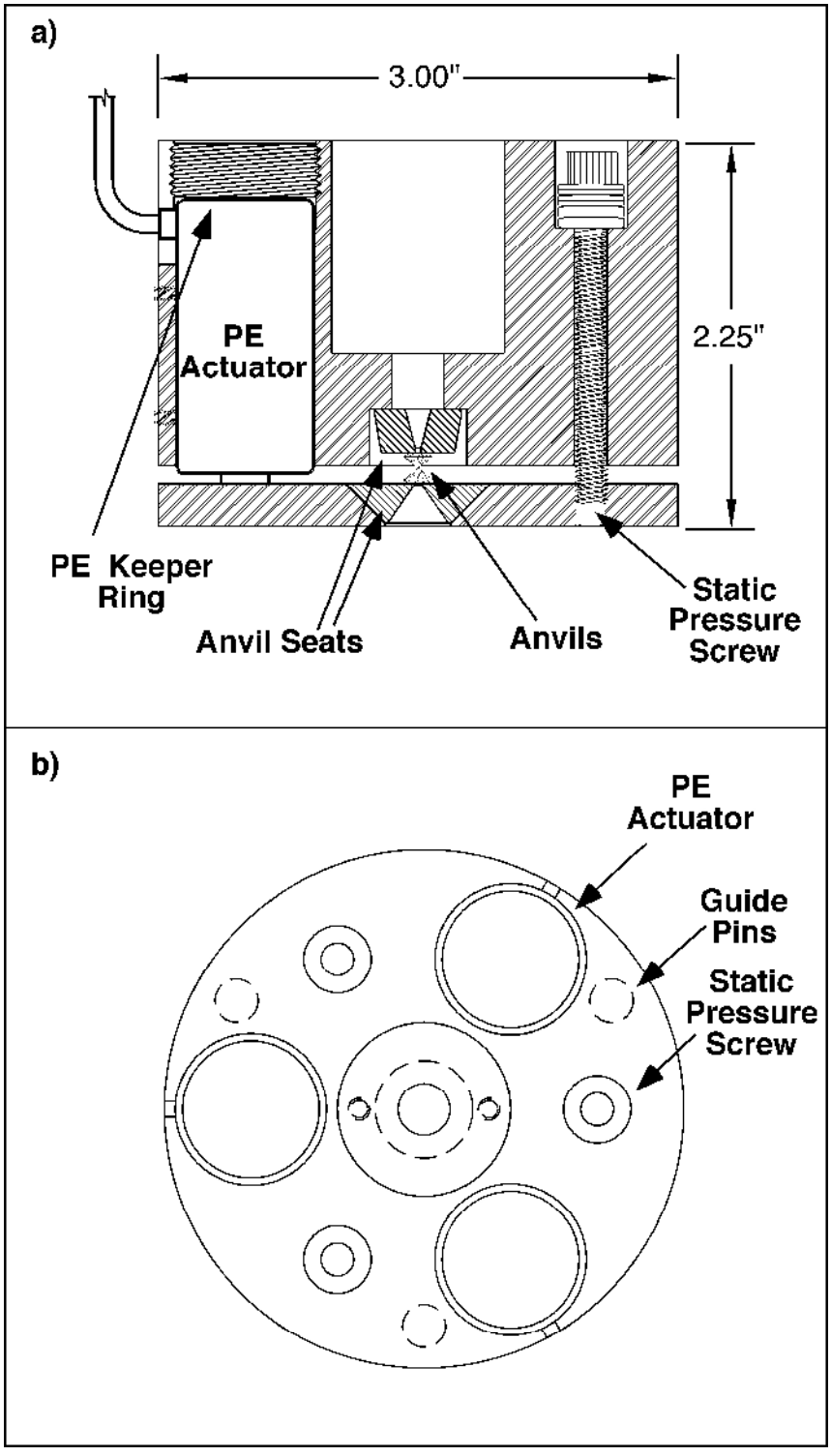
a)
3.00"
2.25"
PE
Actuator
PE Keeper
Ring
Anvil Seats
Anvils
Static
Pressure
Screw
b)
PE
Actuator
Guide
Pins
Static
Pressure
Screw

Figure 2

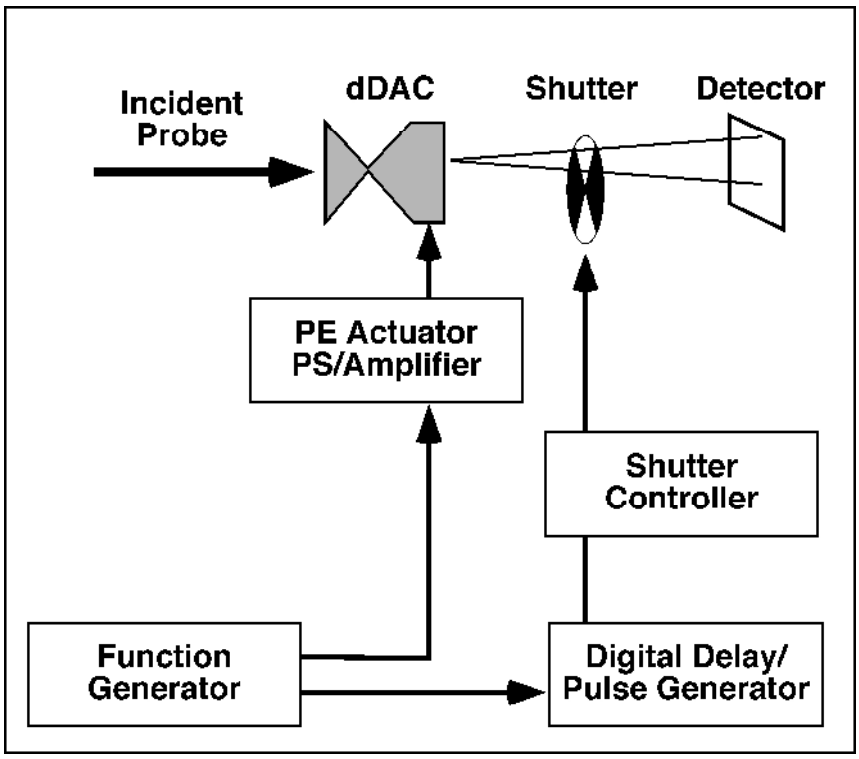
Incident
Probe
dDAC
Shutter
Detector
PE Actuator
PS/Amplifier
Shutter
Controller
Function
Generator
Digital Delay/
Pulse Generator

Figure 3

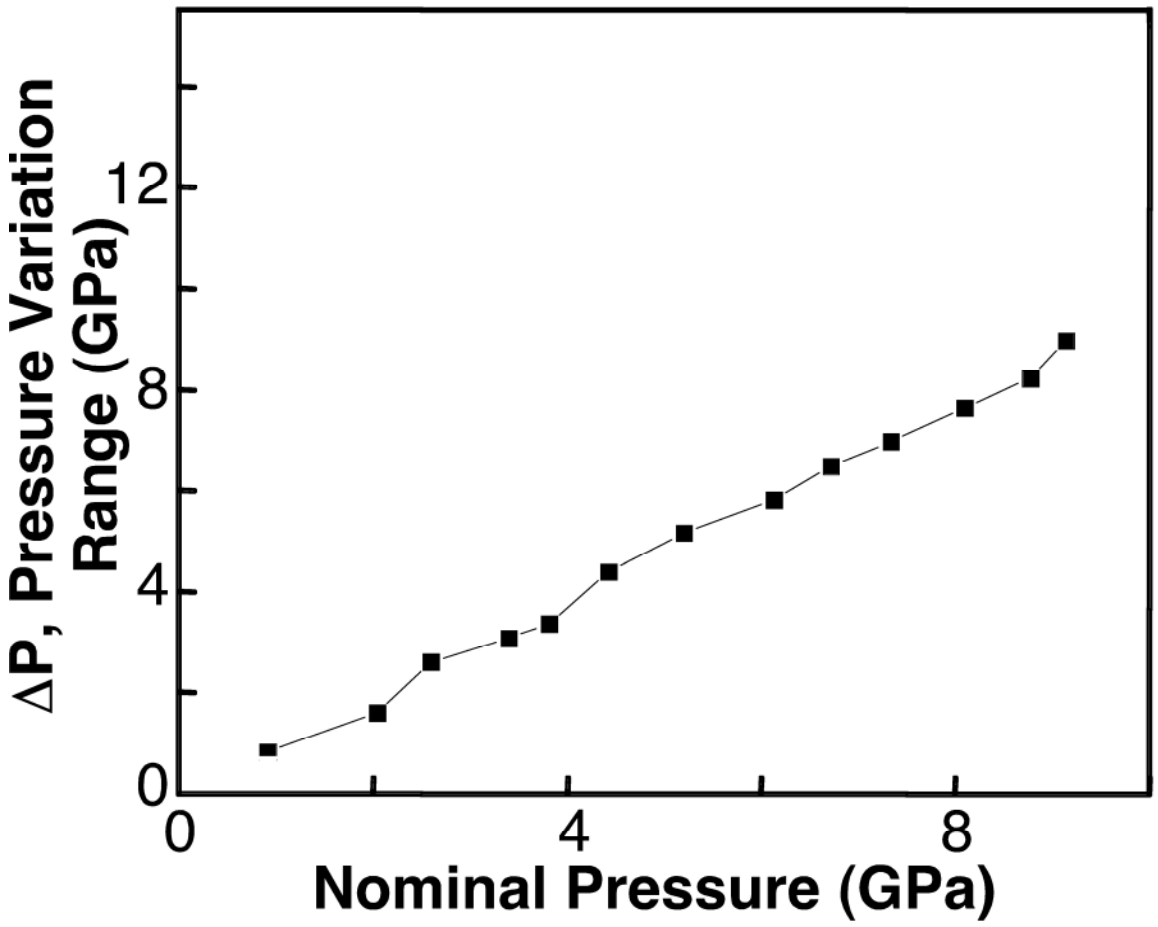
ΔP, Pressure Variation Range (GPa)
0
4
8
12
0
4
8
Nominal Pressure (GPa)

Figure 4

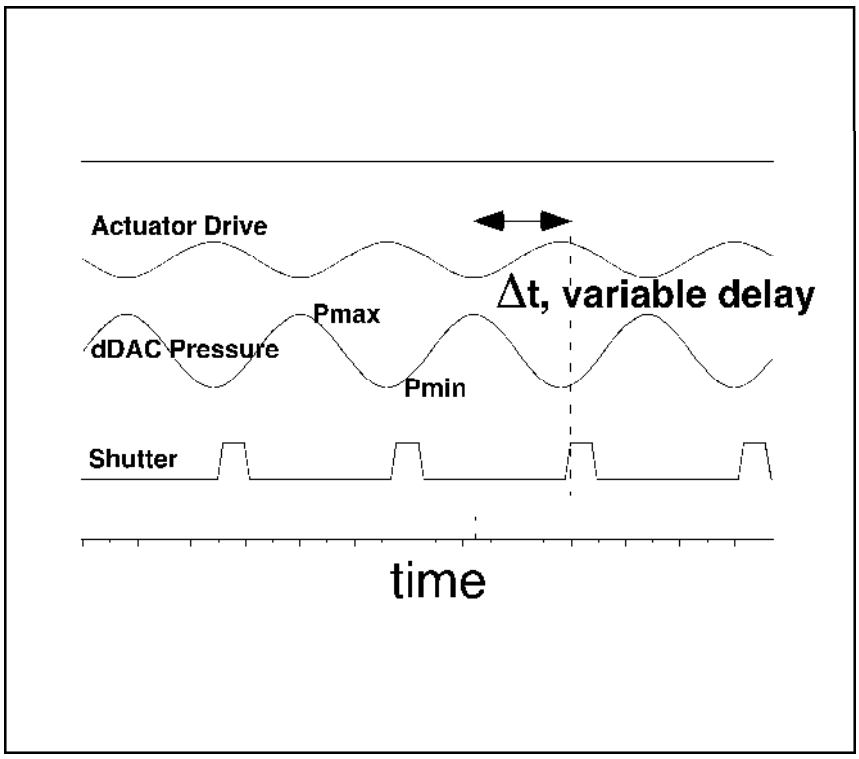
Actuator Drive
Δt, variable delay
Pmax
dDAC Pressure
Pmin
Shutter
time

Figure 5

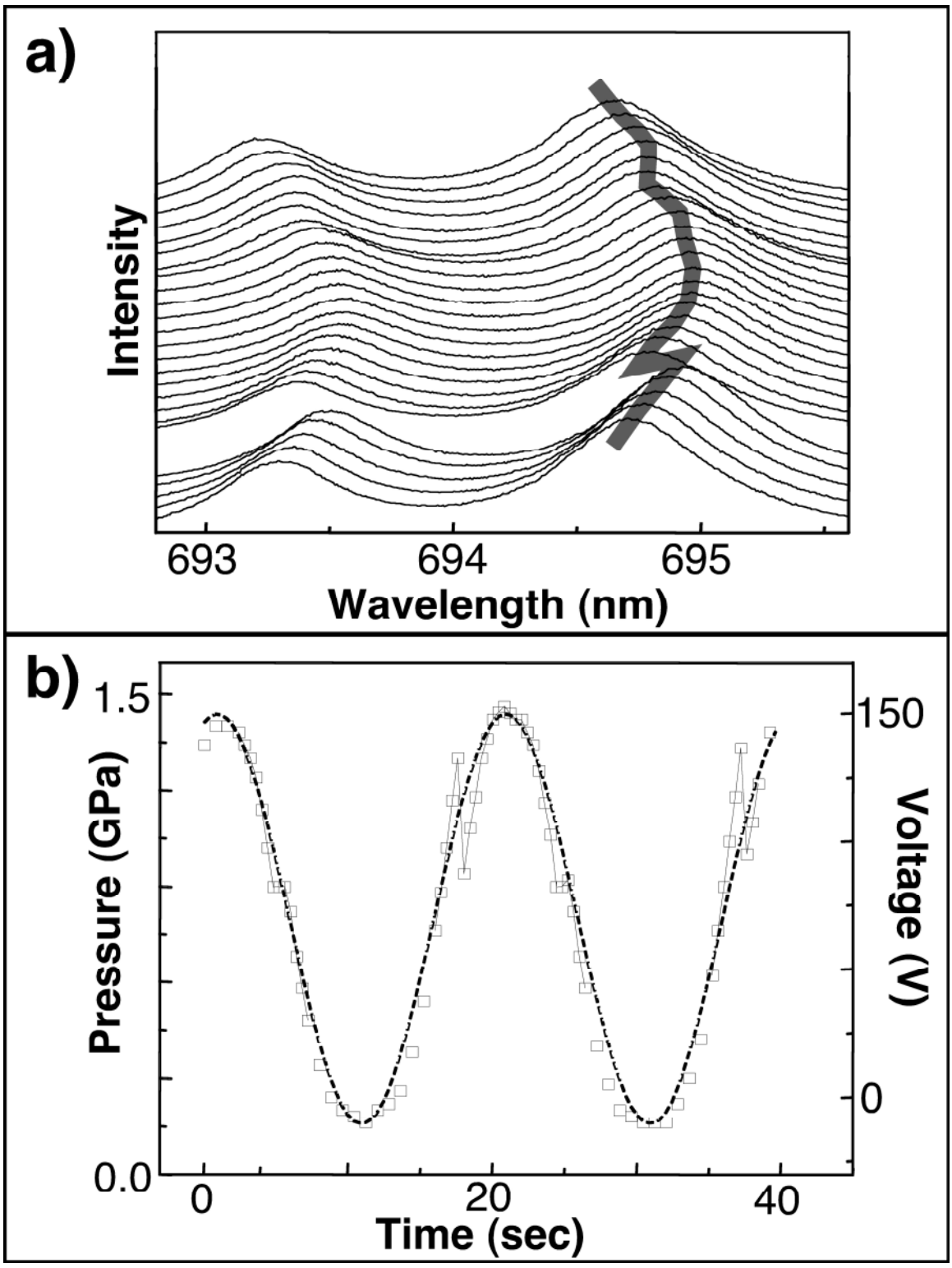
a)
Intensity
693
694
695
Wavelength (nm)
b)
1.5
0.0
Pressure (GPa)
150
0
Voltage (V)
0
20
40
Time (sec)

Figure 6

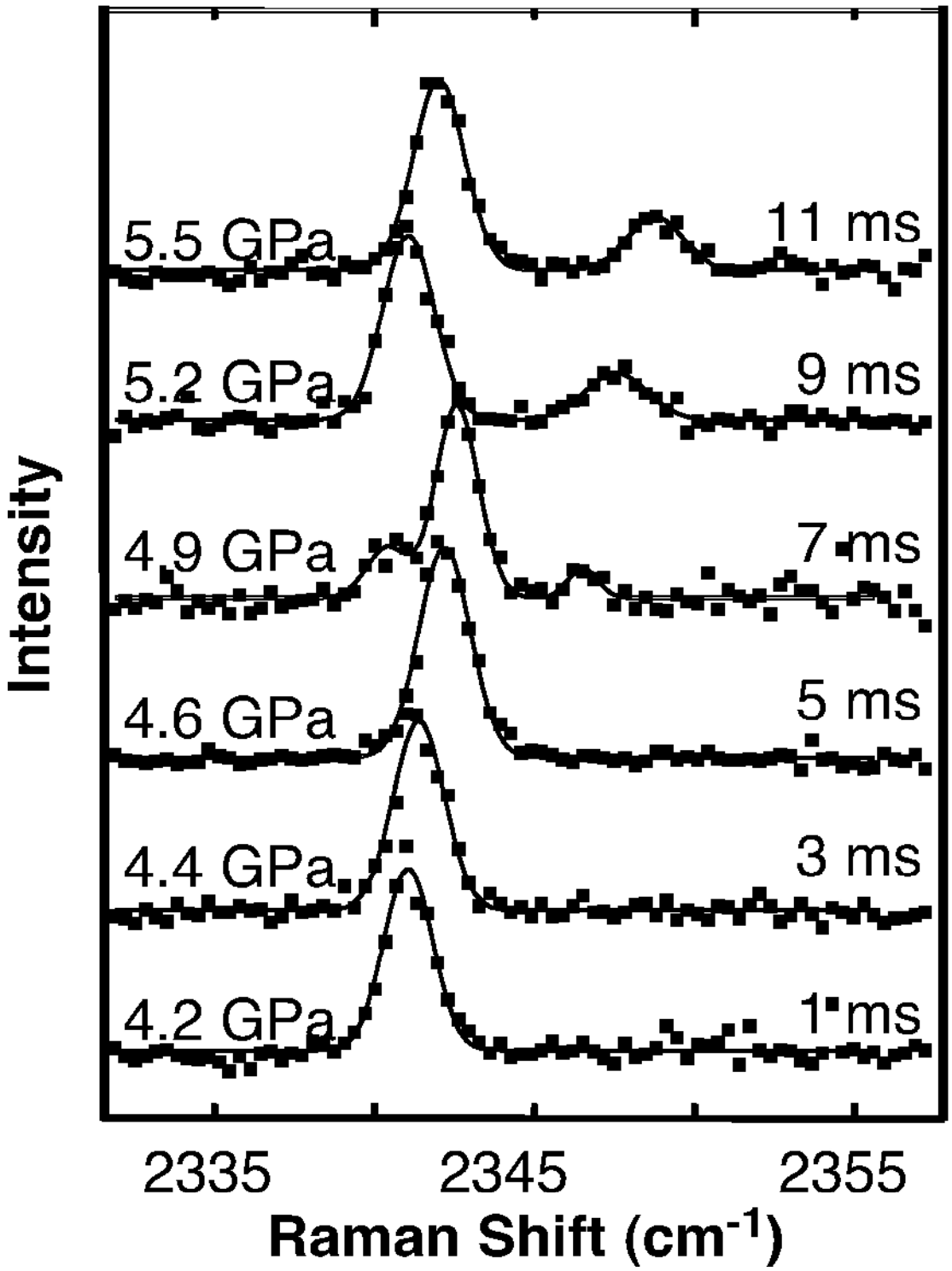
5.5 GPa
11 ms
5.2 GPa
9 ms
4.9 GPa
7 ms
4.6 GPa
5 ms
4.4 GPa
3 ms
4.2 GPa
1 ms
Intensity
2335
2345
2355
Raman Shift (cm-1)

Figure 7

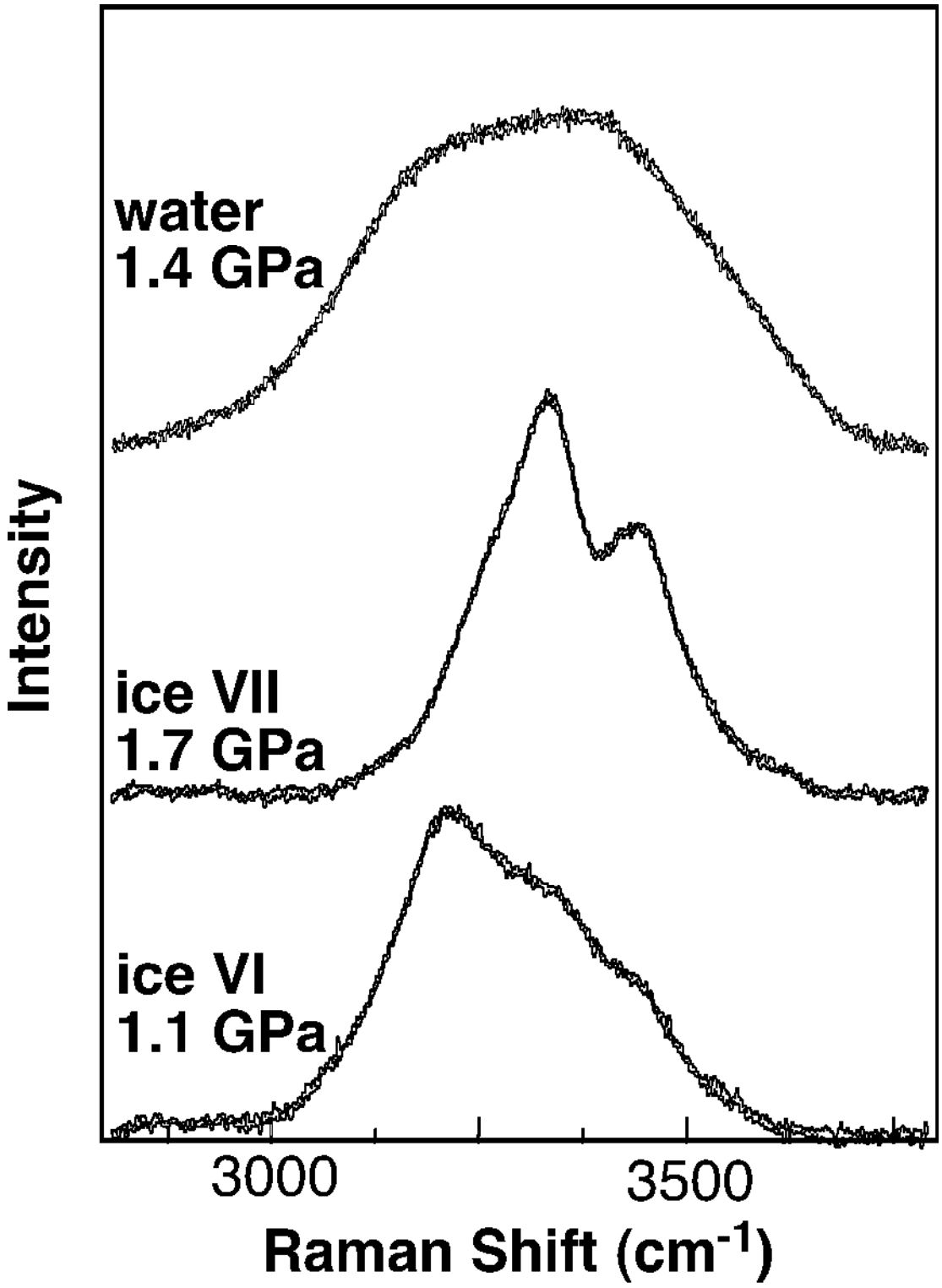
water
1.4 GPa
ice VII
1.7 GPa
ice VI
1.1 GPa
Intensity
3000
3500
Raman Shift (cm-1)

Figure 8